IOP Publishing Journal of Micromechanics and Microengineering
J. Micromech. Microeng. **25** (2015) 085004 (8pp) doi:10.1088/0960-1317/25/8/085004

Self-folding with shape memory composites at the millimeter scale

S M Felton, K P Becker, D M Aukes and R J Wood

Harvard University, 60 Oxford st, Cambridge, MA 02138, USA

E-mail: sam@seas.harvard.edu

Received 20 January 2015, revised 16 April 2015
Accepted for publication 19 May 2015
Published 14 July 2015

Abstract

Self-folding is an effective method for creating 3D shapes from flat sheets. In particular, shape memory composites—laminates containing shape memory polymers—have been used to self-fold complex structures and machines. To date, however, these composites have been limited to feature sizes larger than one centimeter. We present a new shape memory composite capable of folding millimeter-scale features. This technique can be activated by a global heat source for simultaneous folding, or by resistive heaters for sequential folding. It is capable of feature sizes ranging from 0.5 to 40 mm, and is compatible with multiple laminate compositions. We demonstrate the ability to produce complex structures and mechanisms by building two self-folding pieces: a model ship and a model bumblebee.

Keywords: self-folding, shape memory, laminate mechanisms, self-assembly, origami-inspired

S Online supplementary data available from stacks.iop.org/JMM/25/085004/mmedia

(Some figures may appear in colour only in the online journal)

1. Introduction

Origami-inspired engineering is a versatile field with a range of applications. It can be used to deploy complex machines such as folding satellites [1] and solar arrays [2], create stiff, lightweight structures [3], or build sophisticated mechanisms by approximating springs, joints, and rigid elements [4]. It's also an effective means of manufacturing inexpensive machines [5] and devices too small for traditional machining [6].

One branch of this field is self-folding—a fabrication technique in which a flat structure bends itself along hinges, resulting in three-dimensional features [7]. Self-folding has two general categories of applications. The first is in the assembly of structures that are difficult to reach and manipulate. Examples include self-folding inside the body [8], in space [1], or at sizes that are too small for manual manipulation [9]. The second application is to speed up and parallelize foldable structures. For example, a manually folded robot can take up to one hour to fold by hand [5]. A similarly sized self-folding robot can fold itself in approximately five minutes [10].

Various self-folding methods have been demonstrated, actuated by different physical forces including electrostatics [11], differential stress [12], polymer swelling [9, 13], pneumatic pressure [14], and shape memory effects [15, 16]. Each is suited to different applications. For example, Malachowski et al. used differential stress to activate *in vivo* cell grippers because the sacrificial layer could be dissolved in biofluids [8]. Keller used a shape memory alloy to create wires that could tie themselves into knots because each fold could occur in succession [17].

Shape memory composites are self-folding laminates that have been used for creating relatively complex shapes and dynamic machines [10, 18]. Shape memory composites consist of one or more layers of a shape memory polymer (SMP) laminated with one or more structural layers [19, 20]. The SMP is activated by heating, either by light [21], joule heating from embedded resistors [19, 21], or an oven [20, 21], and this induces a contractile stress in the SMP. The substrate is mechanically weakened along hinge lines so that when the SMP contracts and pulls on either side of the hinge, the substrate can fold along the line. This technique has been used to self-fold structures and machines at length scales from 3 to 20 cm [10, 19]. It is capable of both sequential and simultaneous folding, and the laminate construction means different materials can be integrated into the structure [22]. However, these composites are unable to fold features less than one

centimeter in length. On smaller faces, the SMP delaminates from the substrate, preventing folding. We have conducted preliminary research into a new composite that can fold hinges as small as one millimeter [23]. However, the hinges in this composite had to be activated simultaneously due to uniform heating. Additionally, the adhesive used to bond the layers was not adequate, resulting in delamination and imprecise folds.

When selecting a self-folding method for fabrication, there are two major capabilities to consider. The first is whether the method allows for sequential folds. Generally, simultaneously folding all hinges is more reliable, but sequential folding allows for more complex geometries, especially if the folded structure is mechanically coupling to another feature, such as a tab locking into a slot or over a motor shaft [10, 19].

The second capability is the range of length scales that can be folded. The maximum face length limits the overall size of the self-folding structure, while the minimum face size limits the spatial resolution. In addition to absolute size limitations, the ratio between maximum and minimum feature size is important because it correlates with machine complexity. If the maximum length defines the maximum structure size and the minimum length defines the minimum feature size, the ratio indicates the density of features that can be built into the structure.

Previous shape memory composites have only demonstrated a feature length range of 10 to 100 mm [10, 19]. This limited the complexity and minimum size of self-folded devices. In this paper we present an improved shape memory composite capable of folding faces at length scales ranging from 0.5 to 40 mm. This is accomplished through thinner materials, new machining techniques, new adhesion layers, and additional structural layers to prevent delamination. The size reduction of the composite results in a more favorable torque-to-weight ratio, which allows us to experiment with new design parameters. We demonstrate simultaneous folding of an aluminum-based composite activated by a hot plate, and sequential folding of a composite based around a glass-reinforced epoxy (FR-4) and activated by internal resistive heating. We compare the minimum feature size and angular resolution of these designs and demonstrate their efficacy with a resistively heated model ship and a uniformly heated model bumblebee.

2. Design and fabrication

The composite consists of three different materials in seven layers (figure 1). In the middle is the flexural layer, a 7.5 μm thick polyimide film (440, Chemplex). On either side of the flexural layer is a sublaminate consisting of the contractile SMP, polyolefin (DU-POF-1000-8, US Packaging and Wrapping), sandwiched between two substrate layers. The layers are bonded together with 5 μm thick acrylic tape (82600, 3M).

Folding is triggered by heat. When an unconstrained SMP sheet is heated above its transition temperatures, it contracts bidirectionally to 25% of its original length and

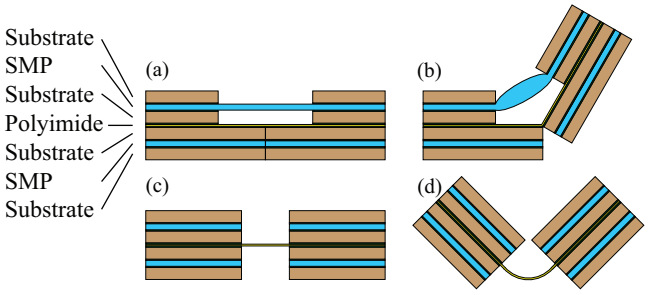

Figure 1. The self-folding composite consists of three functional materials comprising seven layers: the substrate, the polyolefin shape memory polymer (SMP) and the polyimide flexural layer. These are bonded together with an acrylic adhesive. This composite can be programmed with self-folding hinges (a). Folding is induced by activating the SMP, causing it to contract (b). The composite can also be programmed with passive hinges that can bend repeatedly (c) and (d). This figure is adapted from a previous publication [23].

width. However, when embedded in the composite, the SMP is fixed in place by the substrate except along the self-folding hinges, where the SMP is exposed and allowed to contract. This contraction exerts a torque on the hinge, causing it to bend. We can activate this process by supplying heat from an external source, such as a hot plate, or we can embed resistive circuits along each hinge. When we supply these circuits with current they produce heat and locally activate the SMP.

In order to create a self-folding hinge, layer-specific features are machined into the composite (figures 1(a) and (b)). On the concave side of the fold, a gap is cut into both substrate layers to expose the polyolefin and allow it to contract. The width of this gap varies between 0.2 and 1.8 mm, and is correlated with the final fold angle. On the convex side, a line is cut through the substrate and polyolefin layers so that the flexural layer can bend freely. A passive hinge has similar features (figures 1(c) and (d)). A gap is cut in every layer except the flexural layer. In this case, the gap width affects the hinge stiffness and maximum bend angle.

The substrate can be any sufficiently stiff material. In our devices we use two different substrates: aluminum (1145-H19) in the uniformly heated structures and FR-4 (FR408HR, Isola Group) in the resistively heated structures; in both cases the substrate is 50 μm thick. Aluminum was chosen for the uniformly heated structures because of its high stiffness and high thermal conductivity (170 W $m^{-1}K^{-1}$). This enables the entire structure to maintain a uniform temperature even when parts of it lose contact with the hot plate, ensuring that folding continues over the entire structure. In contrast, FR-4 is used in the resistively heated structures because of its low thermal conductivity (0.4 W $m^{-1}K^{-1}$). When folding sequentially, insulation is necessary between adjacent folds to prevent the heat from one hinge from prematurely activating another.

In order to compare the thermal dynamics between substrate materials, we developed a thermal finite element model of two composites, one made with aluminum and one with FR-4. The simulation assumed each hinge was generating heat

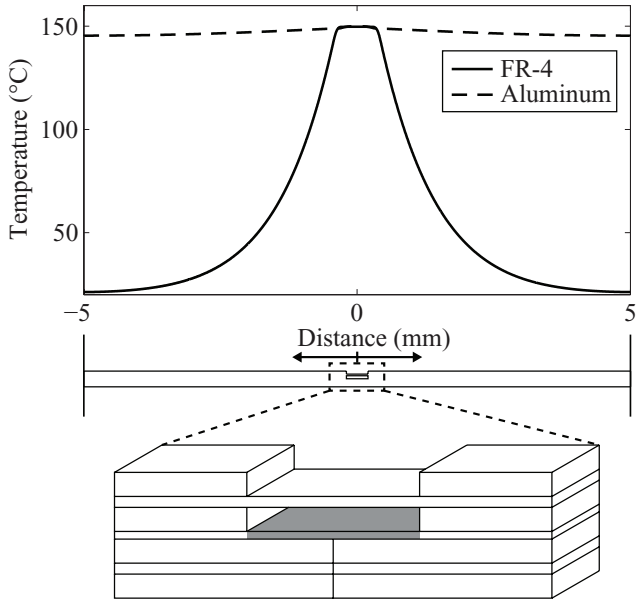

Figure 2. A thermal finite element model of the hinge was built in order to determine the temperature profile of the SMP when the hinge is internally heated to 150 °C. The solid line indicates the temperature profile of the polyolefin when the substrate is FR-4, and the dashed line is the temperature profile when the substrate is aluminum. A diagram of the model hinge is shown below at scale with the graph, and below that a section is blown up to illustrate the hinge geometry. In this figure, the shaded region indicates the volume of the hinge which is generating heat.

at a constant rate, and the polyolefin temperature at the center was approximately 150 °C after 20 s. The temperature profile of the SMP layer orthogonal to the hinge in both situations is shown in figure 2. In the aluminum substrate, the temperature five millimeters from the hinge only dropped to 145 °C, while in the FR-4 substrate the same location is 21 °C. The transition of an SMP often occurs over a 30 °C range [24], so a difference of at least a 30 °C between hinges would be necessary in order to achieve sequential folds.

If the structure requires an embedded circuit, either for resistive heating or for its final function, a copper trace is included on the flexural layer. Copper is used in the devices presented here because it is flexible, easy to sputter coat, and has adequate resistivity for our trace geometry. The copper layer is approximately 200 nm thick; however, we found that our sputtering rate varies between 90 and 200 nm min^{-1}, so the trace thickness varied commensurately. In most hinges (and unless otherwise noted) the resistive portion of the trace is 800 μm wide and runs coincident to the midline of the hinge.

The composites are assembled in steps alternating between laser machining with a diode pump solid-state laser (DC150H-355, Photonics Industries) and bonding (figure 3). First, the two top substrate layers (T1, T2) and the two bottom substrate layers (B1, B2) are prepared by applying the tape to both sides of two layers (T1, B1), and one side of the other two (T2, B2). The tape backing is left on the outer sides of the tape. The features exclusive to the substrate are then machined into the layers. This step uses two different cut patterns: one cut pattern for the substrate layers of the top sublaminate (T1, T2), and one for the layers of the bottom sublaminate (B1, B2). After machining, the polyolefin layers are bonded to T2 and B2 and machined again to remove the polyolefin at the alignment holes. Layers T1 and B1 are then pin-aligned and bonded to the other side of the polyolefin, resulting in the top sublaminate (TS) and bottom sublaminate (BS). Each is machined with another cut pattern, removing material from both the substrate and polyolefin layers. At this point there is adhesive on one side of the TS and BS sublaminates.

Making the flexural circuit layer requires four steps. First, the flexural thin film is rolled onto a piece of Gel-Pak (WF Film, Delphon Industries), which keeps it flat during handling. A mask made of Gel-Pak is cut with the circuit trace pattern and applied with pressure to the flexural layer. It is then sputter-coated with copper for a total of 110 s until the copper layer is approximately 200 nm thick, after which the mask is removed and alignment holes are machined in both the flexural layer and supporting Gel-Pak. If the flexural layer does not include a circuit, the thin film is still attached to the supporting Gel-Pak and machined, but is not masked or sputter-coated.

Once the flexural layer is prepared and the two sublaminates are machined, the TS sublaminate is pin-aligned and bonded to the exposed side of the flexural layer. The supporting Gel-Pak is then removed, and the BS sublaminate is aligned and bonded to the other side. The complete composite is then machined with the release cut pattern, resulting in the final planar structure. This structure is pressed with approximately 2.5 MPa for 45 min. For our resistively heated samples, the composite is secured to a glass slide with double-sided tape and the exposed traces are connected to copper pads with conductive epoxy (8331-14G, MG Chemicals).

3. Model and results

3.1. Maximum feature size

The maximum face length is generally limited by the torque of the hinge, which must overcome the force of gravity on the folding face. We use a previously published model to predict the maximum face size a self-folding hinge can lift [23]. This model assumes that the forces and mechanical behavior of the SMP are quasistatic. We make this assumption because the transient behavior of the SMP is difficult to model. These polymers generally exhibit viscoelastic behavior and undergo large strains, exceeding their linear elastic regime [25]. In addition, their behavior is sensitive to temperature changes, especially within the range over which it transitions from a glass to a rubber phase [24]. In our application the SMP is heated through the transition temperature range quickly (5 to 10 s) and the folding motion usually occurs during the same period, so we ignore the transient material properties. Because of this, we treat the folding as a quasistatic process, and model the SMP, once activated, as if it is in a completely rubber phase with temperature- and time-independent behavior. The stress-strain relationship of the SMP in this state is presented in appendix A. Because of our quasistatic assumption and experimental observations, we can also

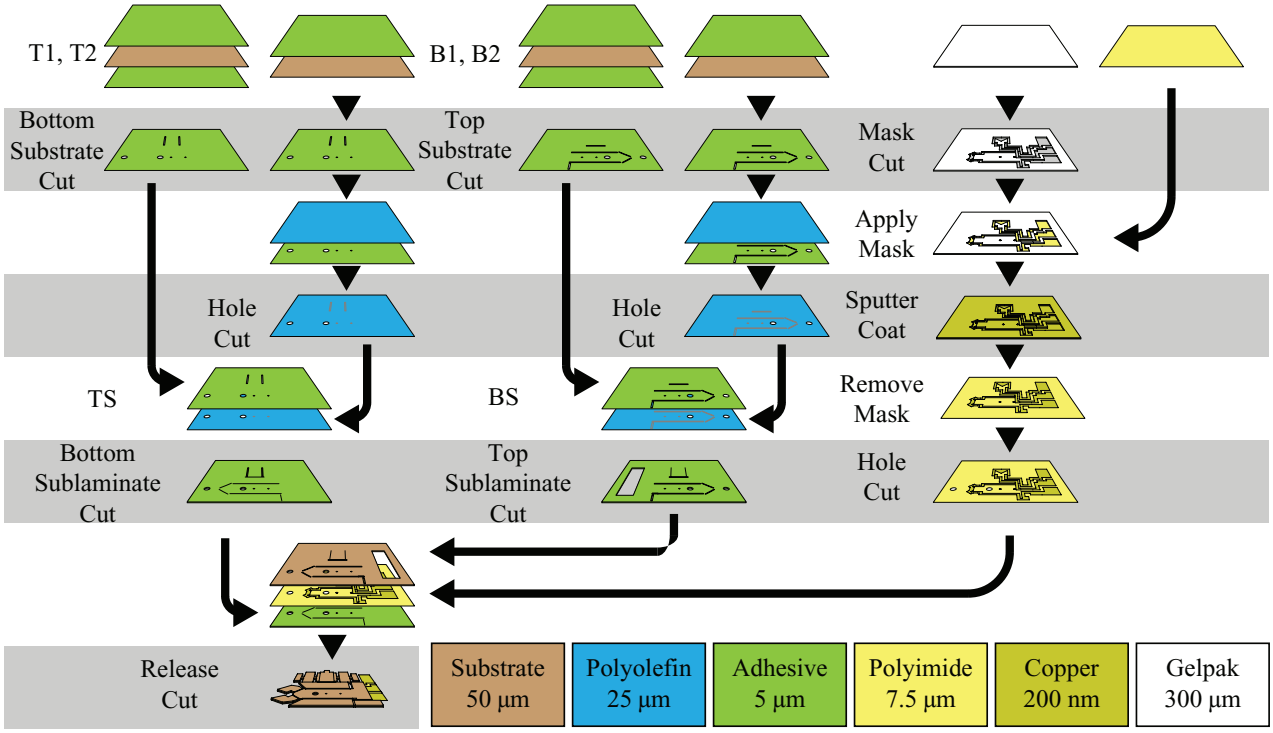

Figure 3. Fabrication occurs in sequential steps alternating between laser machining and bonding layers together.

assume that if the hinge begins to fold, it continues to fold to completion (appendix B). Therefore, we are primarily interested in whether the torque exerted by the SMP in the flat state is enough to overcome gravity and start the folding motion.

The torque induced by the SMP and the weight of the folding face are both linearly proportional to the width of the face, so the ratio between the two is independent of the face width. The torque per meter of hinge length M_s exerted by the SMP is a function of the contractile stress σ, the thickness t_p, and the distance δ_s of the SMP from the bending point. The moment due to gravity per meter hinge length M_g is proportional to the mass m_f of the face and the distance d_f between the hinge and the center of mass of the face. These values are a function of the area density ρ_A, length L_f, and shape of the folding face. Equations (1)–(6) solve for the maximum face length $L_{\max}$ that can be folded with our composite, assuming a rectangular face.

$$M_s = t_p\,\sigma\delta_s \tag{1}$$

$$d_f = L_f/2 \tag{2}$$

$$m_f = \rho_A L_f \tag{3}$$

$$M_g = g\,m_f d_f \tag{4}$$

$$L_f\big|_{M_g=M_s} = L_{\max} \tag{5}$$

$$L_{\max} = \sqrt{2\,t_p\,\sigma\,\delta_s/g\,\rho_A} \tag{6}$$

ρ_A is the sum of the density of each layer multiplied by its thickness. n is the total number of layers, and ρ_i and t_i are the density and thickness of the ith layer, respectively. In our composite, ρ_A depends on t_p, the polyolefin density ρ_p, the substrate thickness t_s and density ρ_s, the polyimide thickness t_h and density ρ_h, and the adhesive thickness t_d and density ρ_d. δ_s is the distance between the SMP and the flexural layer.

$$\rho_A = \sum_{i=1}^{n} \rho_i\,t_i \tag{7}$$

$$= 4\rho_s t_s + 2\rho_p t_p + \rho_h t_h + 6\rho_d t_d \tag{8}$$

$$\delta_s = t_s + t_p/2 + t_h/2 + 2t_d \tag{9}$$

One difference from previous models of shape memory composites is that this paper refers to the contractile stress of the polyolefin. Previous papers referenced the Young's modulus of the SMP and shrink ratio to calculate the contractile stress. However, the mechanical behavior of shape memory polymers can be nonlinear, so it is more accurate to measure the contractile stress directly during transition. This stress was measured to be 5.1 ± 0.3 MPa (appendix A). Other measured values and the expected maximum face lengths for each composite are given in table 1.

We built aluminum test hinges that were 30 mm wide and of varying lengths (30 mm, 40 mm, 50 mm, and 60 mm) to confirm our predictions. These hinges were activated on a hot plate (97042-574, VWR) set to 130 °C. The 30 and 40 mm long faces folded to completion in approximately 15 s, judged by observing a fold of more than 90°, at which point gravity no longer limits the fold angle. The 50 mm and 60 mm long faces took approximately two minutes to stop moving, and neither folded to completion. The 50 mm face stopped at

Table 1. Measured and calculated values for determining maximum face size.

Value	Symbol	Value	Units
Contractile stress	σ	2.5	MPa
Density of polyolefin	ρ_p	1000	kg m^{-3}
Thickness of polyolefin	t_p	25	μm
Density of polyimide	ρ_h	1400	kg m^{-3}
Thickness of polyimide	t_h	7.5	μm
Density of adhesive	ρ_d	1200	kg m^{-3}
Thickness of adhesive	t_d	5	μm
Density of aluminum	ρ_{al}	2700	kg m^{-3}
Density of FR-4	ρ_{fr}	1400	kg m^{-3}
Thickness of substrate	t_s	50	μm
Area density of aluminum composite	ρ_a	636	g m^{-2}
Area density of FR-4 composite	ρ_f	467	g m^{-2}
Lever arm	δ_s	76	μm
Torque per meter	M_s	9.7	mN-m m^{-1}
Max face length—aluminum	L_{max}	56	mm
Max face length—FR-4	L_{max}	65	mm

approximately 46°, and the 60 mm face stopped at approximately 32°. These results underperform our model, which predicted a maximum face length of 56 mm. We believe that this could be due to two factors. Our model ignores the viscoelasticity of the polyolefin in its rubbery state, but the stress relaxation could be a significant part of the material behavior at higher loads. The other possibility is that the higher loads caused the layers in the hinge to delaminate, changing the hinge geometry and blocking folding. In the 50 mm and 60 mm samples we can see signs of delamination, as well as contact between the two folding faces, suggesting that folding stopped when the two sides collided (figure S4).

3.2. Minimum feature size

The minimum face size is generally limited by the ability of composite to resist delamination. In order to determine a minimum feature size, we built experimental hinges with square faces of variable lengths. We first built uniformly heated hinges with an aluminum substrate and faces varying from 0.5 to 3 mm long on a single sample (figure 4(a)). Each hinge had a 400 μm gap width. The completed sample was placed on a hot plate set to 130 °C and left to fold for approximately one minute. These faces all folded successfully. However, there was a noticeable difference in angles, as larger faces folded to sharper angles. We built resistor-heated hinges with FR-4 and faces from one to three millimeters long (figure 4(b)). Smaller faces were not possible because the size of the trace and separating gaps were too fine for our masking process. Because of the small size, the resistive traces were 400 μm wide. These faces also folded successfully when supplied with 100 mA of current (using a 1666 BK Precision power supply). However, they showed greater individual variation in final fold angle. This is likely due to the differences in heat profiles at each hinge; different sized hinges have different edge effects where the traces enter and leave the hinge line. In this case, the smaller faces folded at a lower current than the larger faces. When the current was increased to activate the larger faces, the increased heat led to delamination in the smaller faces.

3.3. Angular control

We used another previously published analytical model to predict final fold angle based on the gap width [23]. This model assumes that the folding stops when the corners of the substrate on either side of the hinge come into contact, producing a quadrilateral (figure 5(a)). Therefore, the fold angle θ is a function of the ratio of the gap width w and composite thickness t and is defined by equation (10).

$$\theta = 2 \arctan(w/t) \tag{10}$$

We built experimental hinges consisting of square faces five millimeters long, attached to a stationary base face. These hinges had gap widths of 0.1, 0.2, 0.4, 0.6, 1.2, and 1.8 mm wide. They were supplied with 180 to 250 mA of current for 20 to 60 s, until folding was completed. This variation is due to the variable resistivity of the heating trace.

The measured fold angles can be seen in figure 5(b) as a function of gap width, along with the analytical model. The model overestimates the final fold angle; we believe this may be due to the substrate increasing in thickness as the SMP contracts and thickens. A thicker composite results in the two faces coming into contact sooner and stopping the folding process prematurely.

We created more experimental hinges with the same geometries and 0.4 mm gap widths. One of these pieces was made with aluminum, and the other was made with an FR-4 substrate, but without the copper traces. Both were uniformly heated on a hot plate set to 130 °C for approximately 15 s. The uniformly heated FR-4 hinges folded to a final angle of 82° with a standard deviation of 1°. This demonstrated more precision than the resistively heated hinges with the same gap width, which had a mean final angle of 90° with a standard deviation of 6°. The aluminum hinges folded to a mean final angle of 122° with a standard deviation of 5°. This increase in angle may be due to the increased rigidity of the aluminum, which would better constrain the polyolefin. Constraining the polyolefin would prevent it from thickening, which in turn would keep the composite thickness from increasing. The standard deviation of the aluminum hinges was less than the standard deviation of the resistively heated hinges with a similar mean fold angle; the resistive hinges with a 0.6 mm gap folded to an angle of 121° ± 8°.

3.4. Demonstration structure: ship

We designed a structure resembling a miniature ship to demonstrate the complexity of a structure folded sequentially via resistive heating (figure 6). This structure assembled through two sequential folding steps (see supplementary video at stacks.iop.org/JMM/25/085004/mmedia). The first folds created the hull of the ship and were activated with 220 mA of

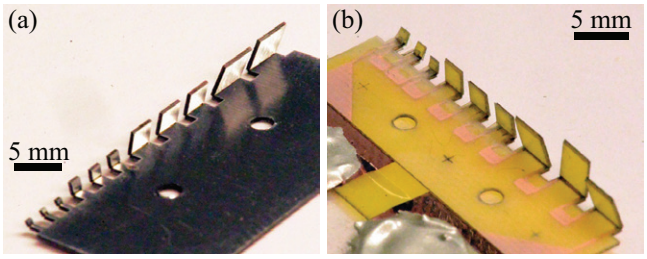

Figure 4. Experimental pieces were built with square faces of variable length to determine the minimum feature size that could be self-folded. (a) A composite with an aluminum substrate was activated by uniform heating from a hot plate, and folded faces from 0.5 to 3 mm in length. (b) A composite with an FR-4 substrate was activated through resistive heating, and successfully folded faces one to three millimeters in length.

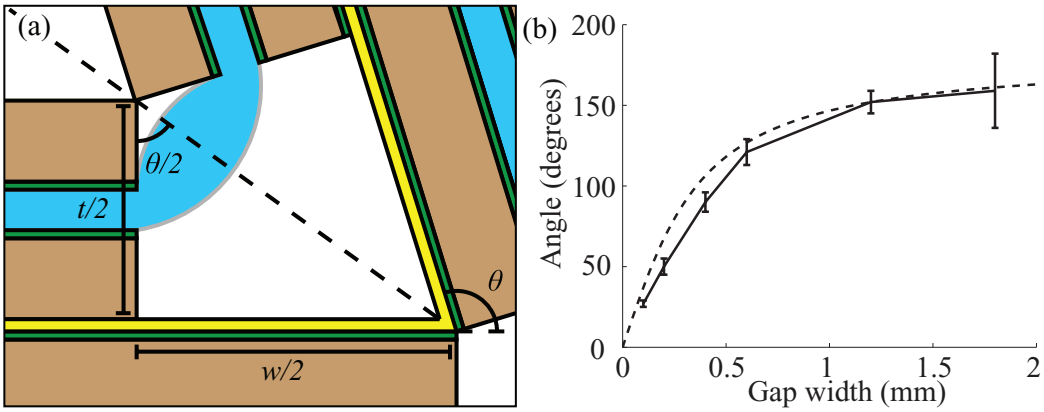

Figure 5. (a) A model for predicting final fold angle based on hinge geometry was developed based on the assumption that folding stopped when the two faces came into contact. The fold angle θ is dependent on the composite thickness t and the width of the gap w cut into the substrate. (b) θ was measured as a function of w (solid line, $N = 8$, error bars indicate standard deviation). These results were compared to an analytical model (dashed line) shown in equation (10).

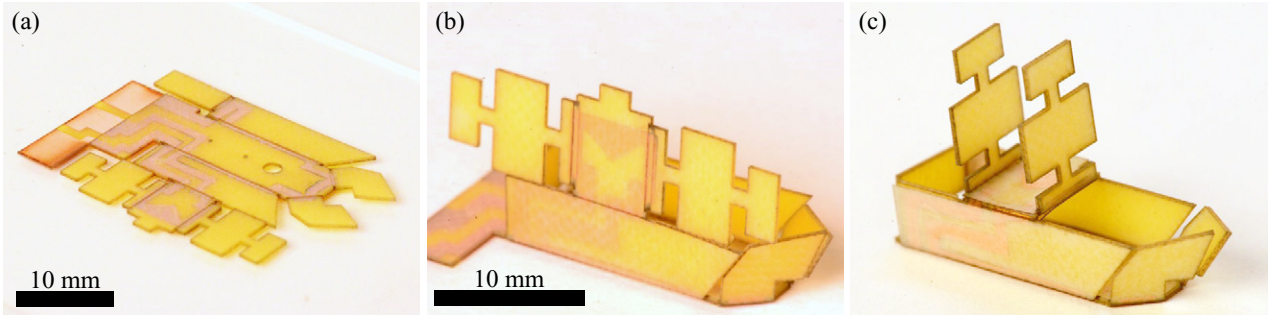

Figure 6. (a) The flat composite programmed to fold into a ship-like structure. (b) The ship after the hull is folded in first folding step. (c) The ship after the sails are folded in the second folding step.

current. The second set raised the sails and was activated with 160 mA. Each step took approximately 20 s. We believe the difference in activating currents may be related to differing thermal profiles in the hinges. The hinges ranged in length from 3 to 13 mm in length, and included both mountain and valley folds.

3.5. Demonstration structure: bumblebee

We designed and built a structure that resembled a bumblebee to demonstrate that uniform folding could produce static structures and dynamic mechanisms (figure 7). The bumblebee assembled during a single folding step (see supplementary video at stacks.iop.org/JMM/25/085004/mmedia) that was activated by a hot plate set to 130 °C. Assembly took eight seconds. This structure includes a self-folding Sarrus linkage which comprises the 'body' of the bee, and wings that are attached to the body via passive hinges. The wings can be actuated by pushing on tabs in the body of the bee. The Sarrus linkage is a single degree-of-freedom mechanism which allows two surfaces to move towards or away from each other while constraining them to remain parallel.

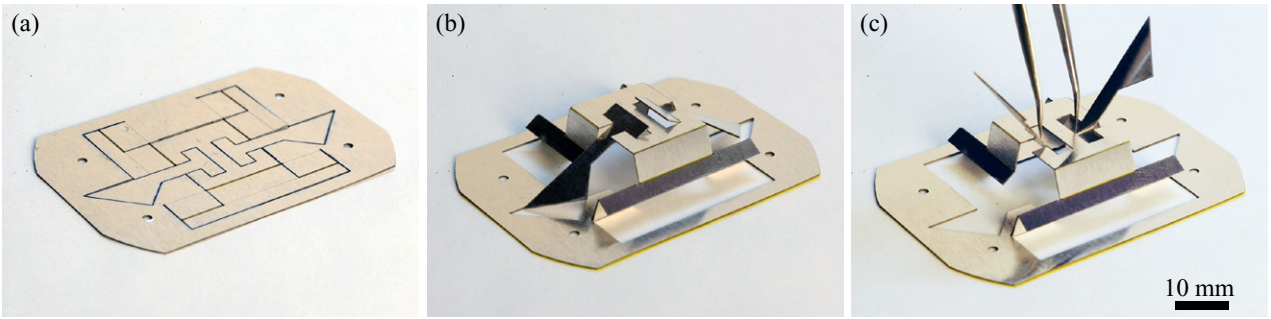

Figure 7. (a) The flat composite programmed to fold into a bumblebee-like structure. (b) The bumblebee after folding. (c) the bumblebee with its wings raised.

This linkage is particularly significant because it forms the basis around which Pop-Up Book MEMS [6, 26] devices are designed, indicating that the self-folding technique presented here is compatible with Pop-Up Book MEMS and could be used to actuate the assembly process. The self-folding hinges ranged in length from 8 to 15 mm in length, and included both mountain and valley folds. The passive hinges were each three millimeters long.

4. Discussion

The self-folding technique presented here demonstrates a way to automate the assembly of structures and machines. This technique is appropriate for features from 0.5 to 40 mm long and is compatible with different materials and activation methods. This is a relatively inexpensive and fast process. For uniformly activated hinges, the only significant piece of equipment needed is a laser cutter with an appropriate resolution. For mass production, the cutting step could be replaced with stamping. Resistively activated hinges also require a means to fabricate the trace, but this was performed without a cleanroom or any hazardous materials.

Previous electrically activated hinges demonstrated an average standard deviation of 6° for hinges folded up to 120° [10], while this new composite exhibited an average standard deviation of 5° for hinges across the same range. It is also capable of achieving a maximum fold angle of 159°, in comparison to a maximum angle of 118° for the previous design [10].

Many centimeter-scale devices are built using folding techniques, including robots [6] and medical tools [27], and this self-folding composite can automate the process. Other devices, such as microfluidic reactors [28] and biochips [29], require 'ship-in-a-bottle' geometries, in which one structure is embedded inside another. Self-folding can be used to assemble a structure even when it is unreachable.

Our results indicate that geometry is not sufficient for predicting hinge behavior. Aluminum hinges exhibit greater fold angles than FR-4 hinges with similar gap widths, which we believe is due to their greater stiffness. In addition, uniformly heated hinges demonstrate greater precision and smaller faces than equivalent resistively heated hinges. This variability may be due to their thermal behavior. These hinges have variable temperature profiles depending on their trace geometry, hinge size, and sputtering process. When this issue is combined with the heat sensitivity of the composite, it can result in delamination and inaccurate fold angles. For instance, the polyolefin used in these experiments has a nominal transition temperature of 130 °C, yet the adhesive has a nominal maximum operating temperature of 150 °C, resulting in a narrow operational range for the composite. If the current is too low, some faces might not fold completely, and if it is too high, other faces might delaminate. When faces delaminate, the joint stops programmed into the composite via gap width are no longer reliable. Unfortunately, the thermal dynamics of these anisotropic systems are difficult to predict. For our experiments the appropriate current for each sample was determined experimentally.

This issue could be corrected by selecting new materials with different thermal properties, or by adjusting individual features of each hinge, such as the supplied current or the trace width. These adjustments would benefit from a thorough characterization of the SMP, the thermal dynamics, and the hinge behavior. The uniformly heated hinges were more precise, but there was still angular variation depending on the hinge length, which also warrants further investigation. Further work can also characterize the mechanical properties of the hinges once folding has ceased. These hinges, while nominally static after cooling, are actually noticeably compliant.

A hot plate was used in these experiments, but this equipment could be replaced with other methods of global heating. Previous methods have already demonstrated that an oven is capable of activating self-folding [20]. Even in an oven, conduction is the primary mode of heat transfer, so the thermal dynamics would be similar to those on a hot plate [23].

It is worth noting that the minimum folded feature length (0.5 mm) is close to the thickness of the composite (0.3 mm). To increase feature resolution, we could combine self-folding with other micromachining techniques. These techniques generally involve etching features into a flat material, so they can only produce features as tall as the thickness of the raw material. In the case of our composite, these techniques could be used to machine features into the surface of the composite up to 0.3 mm in height, while features greater than 0.5 mm could be self-folded. Only features with heights between 0.3 mm and 0.5 mm would be unmachineable by either method.

The folding nature of this method means that it is compatible with computational tools such as Origamizer [30]

and popupCAD [31], as well as mesoscale manufacturing techniques such as Pop-Up Book MEMS [6, 26]. We used popupCAD to design the bumblebee; this has demonstrated the potential of folding-focused computer design tools to speed up our prototyping process. Further work could automate the generation of sequential folding steps, trace patterns, and the control system to supply the necessary currents. We are also interested in integrating electromechanical components such as actuators and sensors into our self-folded mechanisms to produce autonomously folding machines.

By scaling shape memory composites down, integrating new materials, and demonstrating pop-up style folding, these results represent a link between self-folding techniques and fold-based mesoscale manufacturing. Because of the simplicity of fabrication and flexibility with regards to materials and geometry, we believe that this is a valuable method for creating self-folding structures and machines.

Acknowledgments

The authors gratefully acknowledge support from the National Science Foundation (award numbers CCF-1138967 and EFRI-1240383) and the DoD, Air Force Office of Scientific Research, National Defense Science and Engineering Graduate (NDSEG) Fellowship, 32 CFR 168a. Any opinions, findings, and conclusions or recommendations expressed in this material are those of the authors and do not necessarily reflect those of the funding organizations.

References

[1] Zirbel S A, Lang R J, Thomson M W, Sigel D A, Walkemeyer P E, Trease B P, Magleby S P and Howell L L 2013 *J. Mech. Des.* **135** 111005
[2] Tang R, Huang H, Tu H, Liang H, Liang M, Song Z, Xu Y, Jiang H and Yu H 2014 *Appl. Phys. Lett.* **104** 083501
[3] Schenk M and Guest S D 2011 *Origami* **5** 291–304
[4] Lee D Y, Jung G P, Sin M K, Ahn S H and Cho K J 2013 *IEEE Int. Conf. on Robotics and Automation* (*Karlsruhe, Germany*, *6–10 May*) pp 5612–7
[5] Onal C D, Tolley M T, Rus D and Wood R J 2014 *IEEE/ASME Transactions on Mechatronics* to be published (doi:10.1109/TMECH.2014.2369854)
[6] Sreetharan P S, Whitney J P, Strauss M D and Wood R J 2012 *J. Micromech. Microeng.* **22** 055027
[7] Leong T G, Zarafshar A M and Gracias D H 2010 *Small* **6** 792–806
[8] Malachowski K, Jamal M, Jin Q, Polat B, Morris C J and Gracias D H 2014 *Nano Lett.* **14** 4164–70
[9] Na J H, Evans A A, Bae J, Chiappelli M C, Santangelo C D, Lang R J, Hull T C and Hayward R C 2015 *Adv. Mater.* **27** 79–85
[10] Felton S, Tolley M, Demaine E, Rus D and Wood R 2014 *Science* **345** 644–6
[11] Ahmed S, Ounaies Z and Frecker M 2014 *Smart Mater. Struct.* **23** 094003
[12] Bassik N, Stern G M and Gracias D H 2009 *Appl. Phys. Lett.* **95** 091901
[13] Guan J, He H, Hansford D J and Lee L J 2005 *J. Phys. Chem.* B **109** 23134–7
[14] Niiyama R, Rus D and Kim S 2014 *IEEE Int. Conf. on Robotics and Automation* (*Hong Kong, China*, *31 May–7 June*) pp 6332–7
[15] Hawkes E, An B, Benbernou N M, Tanaka H, Kim S, Demaine E D, Rus D and Wood R J 2010 *Proc. Natl Acad. Sci.* **107** 12441
[16] Liu Y, Boyles J K, Genzer J and Dickey M D 2012 *Soft Matter* **8** 1764–9
[17] Keller S L 2004 *Am. J. Phys.* **72** 599–604
[18] Felton S M, Tolley M T, Onal C D, Rus D and Wood R J 2013 *IEEE Int. Conf. on Robotics and Automation* (*Karlsruhe, Germany*, *6–10 May*) pp 277–82
[19] Felton S M, Tolley M T, Shin B, Onal C D, Demaine E D, Rus D and Wood R J 2013 *Soft Matter* **32** 7688–94
[20] Tolley M T, Felton S M, Miyashita S, Aukes D, Rus D and Wood R J 2014 *Smart Mater. Struct.* **23** 094006
[21] Tolley M T, Felton S M, Miyashita S, Xu L, Shin B, Zhou M, Rus D and Wood R J 2013 *IEEE/RSJ Int. Conf. on Intelligent Robots and Systems* (*Tokyo, Japan*, *3–8 November*) pp 4931–6
[22] Shin B, Felton S M, Tolley M T and Wood R J 2014 *IEEE Int. Conf. on Robotics and Automation* (*Hong Kong, China*, *31 May–7 June*) pp 4417–22
[23] Felton S M, Tolley M T and Wood R J 2014 *IEEE Int. Conf. on Automation Science and Engineering* (*New Taipei, Taiwan*, *18–22 August*) pp 1232–7
[24] Tobushi H, Okumura K, Hayashi S and Ito N 2001 *Mech. Mater.* **33** 545–54
[25] Mather P T, Luo X and Rousseau I A 2009 *Annu. Rev. Mater. Res.* **39** 445–71
[26] Whitney J P, Sreetharan P S, Ma K Y and Wood R J 2011 *J. Micromech. Microeng.* **21** 115021
[27] Gafford J B, Kesner S B, Wood R J and Walsh C J 2013 *ASME Proc. 37th Mechanisms and Robotics Conf. (Portland, OR, 4–7 August)* DETC2013-13086
[28] Masuda M, Sugioka K, Cheng Y, Hongo T, Shihoyama K, Takai H, Miyamoto I and Midorikawa K 2004 *Appl. Phys.* A **78** 1029–32
[29] Wu D, Wu S Z, Xu J, Niu L G, Midorikawa K and Sugioka K 2014 *Laser Photonics Rev.* **8** 458–67
[30] Tachi T 2010 *IEEE Trans. Vis. Comput. Graphics* **16** 298–311
[31] Aukes D M, Goldberg B, Cutkosky M R and Wood R J 2014 *Smart Mater. Struct.* **23** 094013